Laser-induced electronic desorption from InP surfaces studied by femtosecond nonresonant ionization spectroscopy

J. Kanasaki,* N. Mikasa, and K. Tanimura†
Department of Physics, Graduate School of Science, Nagoya University, Furo-cho, Chikusa, Nagoya 464-8602, Japan
(Received 5 October 2000; published 26 June 2001)

Laser-induced desorption from clean surfaces of InP(110)-(1×1) and InP(100)-(4×2) has been studied for laser fluences well below melt and ablation thresholds. For detecting desorbed neutral species simultaneously with high sensitivity, we used femtosecond nonresonant ionization spectroscopy with a detection limit as low as the order of 10^{-7} monolayers per pulse. Species desorbed are P, P_2, and In, the relative yields of which are strongly dependent on the surface structures, and the efficiencies of desorption for the three species are superlinear with respect to the excitation intensity. Desorption yields of all species decrease with increasing number of laser shots on the same spot, suggesting desorption from preexisting surface defect sites. Time-of-flight measurements for P, P_2, and In from InP surfaces revealed that the peak flight time and the velocity distribution did not depend on the excitation intensities. The mechanism of the laser-induced desorption is discussed based on these results.

DOI: 10.1103/PhysRevB.64.035414 PACS number(s): 79.20.Ds, 61.80.Ba, 78.66.Fd, 68.35.Ja

I. INTRODUCTION

The interaction of laser light with semiconductor surfaces has been studied extensively. Ejection of constituent atoms and ions from surfaces are often induced by the interaction, and the process is referred to as laser-stimulated desorption (LSD). The phenomena have been studied for several kinds of semiconductors and for a variety of laser light sources with different characteristics.[1] For example, even when we restrict ourselves to nanosecond laser excitation of the surface, the fluence range that can cause desorption is from a few hundreds of μJ/cm^2 to a few J/cm^2 with wavelengths ranging from ultraviolet to near infrared. As clearly demonstrated, the surfaces of semiconductors start to melt upon laser irradiation above certain thresholds of fluence, which depend on the wavelength, pulse width, and basic properties of substance.[2] Sublimation of constituent atoms from laser-induced molten layers is a well-established mechanism for laser fluences above the melt threshold.[3] At greater fluence regimes, the interaction of laser pulses with a surface can cause ablation, in which a dense plasma is formed to cause ejection of highly energetic ions and atoms. On the other hand, desorption of constituent atoms can be induced in some systems even for fluence ranges much below the thresholds of melting and ablation.[4–9] Some LSD phenomena below the melt threshold have been ascribed to the thermal mechanism in which sublimation takes place from the laser-heated layers.[6] However, recent studies of scanning tunneling microscopy observation of the laser-irradiated surfaces have demonstrated that the removal of atoms that are incorporated in the reconstructed structures of semiconductor surfaces can take place electronically.[9,10]

The LSD below melt thresholds were studied for several *MX* compound semiconductors (where *M* and *X* denote, respectively, metallic and nonmetallic elements). In earlier work, quadrupole-mass spectrometers (QMS) were the primary tool used for detecting emitted neutral species.[4–7] In these studies, it has been shown that monatomic (X) and diatomic (X_2) nonmetallic species are emitted as major products, together with monatomic metallic species (M), and that yields of these neutral species commonly show a highly superlinear dependence on the laser fluence. Several models of the electronic mechanism of laser-induced desorption were proposed based on these results.[4,5,7] However, for establishing a basic understanding of the electronic mechanism of LSD, the following aspects need clarification: (1) the electronic transition that triggers the desorption, (2) the initial bonding properties of atoms to be desorbed, and (3) the origin of the instability that causes bond breaking and desorption, as has often been pointed out in the studies of desorption induced by electronic transition.[11] From this point of view, studies by means of QMS usually have two serious drawbacks; both of which are related to the poor sensitivity of this method of detection. For observing desorbates with a reasonable signal-to-noise ratio with QMS, one must remove typically a few monolayers (ML's) per laser pulse. Therefore, desorption always takes place at highly damaged structures of the surface region. For such cases, it is difficult not only to identify the initial bonding configurations of atoms to be desorbed, but also to specify electronic transitions responsible for the desorption processes. Therefore, the poor sensitivity of QMS gives us less than ideal situations to analyze the results to reveal primary processes responsible for the bond breaking and desorption. The second drawback is concerned with the gas-phase dynamics after desorption. As analyzed theoretically, the densities of laser-induced desorbed particles per unit volume per unit time in vacuum were high enough to induce collisions among emitted species, leading to the formation of Knudsen layer.[12] By this process after desorption, several important characteristics of the desorption process were lost or modified significantly. Thus, for understanding the mechanism of LSD, detection methods with much higher sensitivity are highly desired for detecting neutral species.

Recently, LSD from semiconductor surfaces was studied by using a highly sensitive resonance ionization spectroscopy (RIS), in which neutral species emitted were ionized by

 ©2001 The American Physical Society

nanosecond laser pulses via resonance-enhanced multiphoton absorption processes.[7–9,13] However, the method has been applied mainly for metallic neutral species desorbed from the surfaces of compound semiconductors. Very few applications of the RIS have been reported for nonmetallic species that have higher ionization potentials[13] because of some experimental difficulties; it is not conventional to generate intense nanosecond laser pulses at appropriate photon energies in the ultraviolet region. Although the studies by means of RIS have revealed some interesting aspects of LSD, it is not enough to obtain full information of the desorption process, since the important knowledge of the nonmetallic species has been completely absent in some cases, or has been obtained only in the higher-fluence regime.[13] Therefore, a new detection method, which is sensitive enough for both metallic and nonmetallic species, should be employed for establishing the understanding of the primary processes of LSD from compound semiconductor surfaces.

In this paper, we report the laser-induced desorption from clean InP surfaces by means of femtosecond nonresonant ionization spectroscopy (FNRIS),[14,15] in which all neutral species desorbed by a single laser pulse are ionized by intense femtosecond laser pulses and detected simultaneously. Surfaces of InP with the different crystal faces of (100) and (110) were prepared and characterized carefully by low-energy-electron diffraction (LEED) and Auger-electron spectroscopy (AES). The species desorbed from InP are P, P_2, and In, the relative intensities of which are strongly dependent on the surface structure. The efficiency of the desorption is superlinear with respect to the excitation intensity, and the yields of desorption of all these species decrease with increasing number of laser shots on the same spot, suggesting the desorption originates from preexisting surface defect sites. Possible mechanisms of LSD from InP surfaces are discussed below based on these results.

II. EXPERIMENT

Specimens with a (100) crystal face were cut from a wafer of *n*-type InP to the dimensions of 10 mm×15 mm×0.5 mm. Specimens with a (110) crystal face were obtained by cleaving a crystal block of *n*-type InP in air to 10 mm×15 mm ×1 mm in size. These were cleaned by ultrasonically rinsing in ethanol and then were mounted onto a Ta holder in an ultrahigh vacuum (UHV) chamber with a base pressure of 5×10^{-11} Torr. Then, a standard procedure was applied for obtaining clean surfaces by Ar^+-ion sputtering and heating. After several cycles of the treatments, InP(100) and InP(110) surfaces exhibited sharp (4×2) and (1×1) LEED patterns, respectively. No contaminants were detected by AES.

Laser pulses of 6-ns temporal widths were generated for exciting the surfaces with a Nd:YAG-laser pumped dye laser (YAG denotes yttrium aluminum garnet) (Lambda Physik, Spectramate 2B). We mainly used 460-nm laser pulses in this study, since the photon energy falls in resonance with one of the surface-specific optical transition bands of InP(110)-(1×1) revealed by surface reflectance spectroscopy.[16,17] Putting appropriate neutral-density filters on the optical path controlled intensities of the excitation-laser pulses. The laser beam was focused to 1-mm diameter on the surface by a quartz lens (350-mm focal length), and the intensity of each pulse was monitored by a calibrated photodiode (Hamamatsu, Model No. S1337-1010 BQ). The fluence on the surface was evaluated by the energy per pulse and irradiation radius at which the beam intensity decreases from the peak intensity to $1/e$.

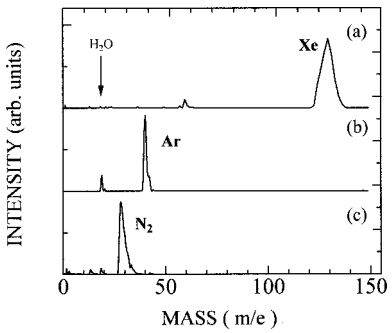

FIG. 1. Mass spectra measured for (a) Xe, (b) Ar, and (c) N_2, partially filled in the chamber. These neutral gases were ionized by femtosecond laser pulses of 800 nm with energy of 2 mJ/pulse. The peak at m/e of 18 can be assigned to residual H_2O in the chamber, and some other peaks were detected below an m/e of 30.

The neutral atoms ejected from surfaces were detected by means of the FNRIS technique. Femtosecond laser pulses of 800 nm with a temporal width of 120 fs were generated with a regenerative-amplified Ti:saphire laser system (BMI Alpha-10). The laser pulses for ionizing desorbed neutral species were guided to pass parallel to the sample surface at a distance of 2.0 mm. Ions ionized by laser pulses were collected by a negatively biased (−120-V) drift tube, and then they were detected by a microchannel plate placed in a shield box located behind the drift tube. The output of the detecting electronics was stored in microcomputer via an analog-to-digital converter. Time-of flight (TOF) spectra of desorbed species were measured by changing the time delay of the pulses for ionization with respect to the incidence of nanosecond laser pulses for surface excitation by using a delay generator (Stanford Research Instrument, Model No. DG-535).

III. EXPERIMENTAL RESULTS

A. Characteristics of the FNRIS technique

First, we describe the basic characteristics of our FNRIS method used in this study. In order to estimate the sensitivity and mass resolution of this detection method of neutral species, we measured ionization efficiencies of several neutral gases at partial pressures of less than 10^{-7} Torr. In Fig. 1 are shown the mass spectra measured for Ar, Xe, and N_2 ionized by femtosecond laser pulses of 2 mJ. For each spectrum, it is evident that Ar^+, Xe^+, and $N_2{}^+$ ions are clearly detected at the positions expected, although some unknown peaks are also detected for m/e less than 30. Since H_2O (m/e of 18) can be detected, we presume that these peaks are due to residual gases in the chamber. It should be noted in Fig. 1(c) that almost no N^+ signals were detected for ionization of N_2 molecules. This indicates that the rate of dissociative ioniza-

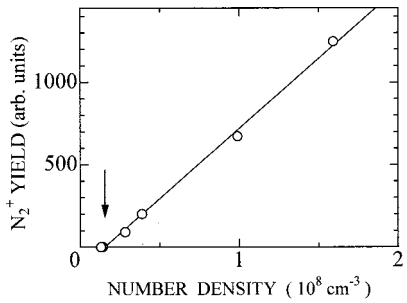

FIG. 2. The relation between ion signals and the number density of N_2 molecules. Femtosecond laser pulses with energy of 2 mJ ionized N_2 molecules.

tion of N_2 molecules can be neglected, compared with simple ionization of N_2. Since N_2 and P_2 are isoelectronic, we may expect a similar result for P_2 molecules. This gives us an additional advantage of simultaneous detection of all possible desorbed neutral species from InP, since the determination of desorption yield of monatomic P is not disturbed by the dissociative ionization of P_2 which is known as one of the desorbed species in LSD from InP surfaces.[13]

In order to evaluate the sensitivity of our FNRIS system, ion signals of N_2 molecules were measured as a function of the partial pressure of N_2 and of the intensity of ionization pulses. For a given partial pressure of N_2, the ion signals were found to increase with increasing intensity of ionization laser pulses. The ion signal was roughly proportional to the 10th power of laser intensity, although the ion signal did not show saturation even for the highest intensity of 2.5 mJ/pulse in our system. In Fig. 2, we show the intensity of N_2^+ signals as a function of number density of N_2 molecules. For the intensity of ionization laser pulse of 2 mJ, the ion signal can be detected clearly above the number density of $1.6 \times 10^7/\mathrm{cm}^3$. When we take into account the ionization volume, which was approximated as a cylinder with a diameter of 0.2 mm and a length of 1 mm, then the number of N_2 molecules in this volume amounts to 5×10^2 molecules, which is the lower bound to be detected by FNRIS.

For evaluating the absolute sensitivity of this FNRIS method in the desorption study, we need to examine carefully several characteristics of desorption processes.[14,15] Evidently, the angular and velocity distributions of desorbed neutral species govern the amount of the neutral species that flow into the ionization volume after desorption. Also, the probability of ionizing these neutral species by a femtosecond laser pulse is also an important factor. Here, as a crude guide of the sensitivity of our FNRIS technique, we consider the simplest case where desorption of neutral species takes place with a rectangular form of velocity distribution and without any preferential angular distribution. In such a case, the solid angle Ω of the ionization volume and the fraction ρ of the neutral species lying in the ionization volume, relative to the whole spatially distributed neutral species along the direction normal to the surface, at a given delay time after excitation can be taken as the main factors that determine the sensitivity. The magnitudes of these factors can be estimated $\Omega\approx1\times10^{-2}$ and $\rho\approx5\times10^{-2}$ under the present experimental conditions.[18] Therefore, by assuming the probability of ionizing the neutral species to be unity, the lower bound of desorbed neutral species per pulse is estimated to be $5\times10^2/\rho\Omega=1\times10^6$ neutral species. Since surfaces are excited by laser pulses with a beam diameter of 1 mm, this amount of neutral species corresponds to 10^{-7} ML, which is almost comparable to the sensitivity of RIS applied for Si.[9] The estimation described above, though crude, indicates that FNRIS can be a powerful method to detect neutral species desorbed from surfaces simultaneously with high sensitivity.

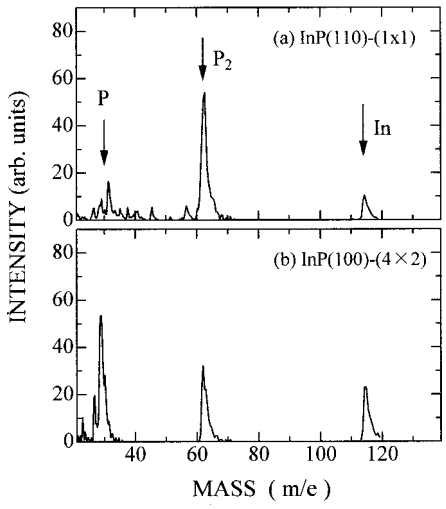

FIG. 3. Mass spectra of desorbed species from laser-excited (a) InP (110)-(1×1) and (b) InP (100)-(4×2). Both InP surfaces were excited by nanosecond laser pulses of 460 nm with a fluence of 48 $\mathrm{mJ/cm}^2$, and desorbed neutral species were ionized by femtosecond laser pulses (800 nm, 2 mJ). The time delay between nanosecond laser pulses for surface excitation and (fs) femtosecond laser pulses for ionizing neutral species was set at 5.5 μs for both surfaces. Three arrows in the figure indicate the positions for monatomic P and P_2 molecules and In atoms, respectively.

B. Laser-induced desorption from InP surfaces

In Figs. 3(a) and 3(b), we show, respectively, the mass spectrum of neutral species desorbed by the excitation with 460-nm laser pulses for InP(110)-(1×1) and InP(100)-(4×2) surfaces. Both spectra were measured at a 5.5-μs time delay of ionization laser pulses. In the figures, three arrows at the position of m/e of 115, 62, and 31 correspond to monatomic In, diatomic P_2, and monatomic P, respectively. We presume that some peaks detected in the region with m/e less than 30 in the spectra originate from residual gasses, since they could be detected even when the surfaces of InP were not excited. These background peaks made it difficult to detect monatomic P desorbed when the intensity was small as in the case of InP(110). However, as seen in Fig. 3(b), the P signal is clearly distinguished from the background for the InP(100) surface. It is evident that the relative ratio of these desorbed species depends strongly on the surfaces; P_2 is the major product from InP(110), whereas P dominates over other species for InP(100).

The yields of these neutral species were measured first as a function of the number (n) of laser shots at the same spot

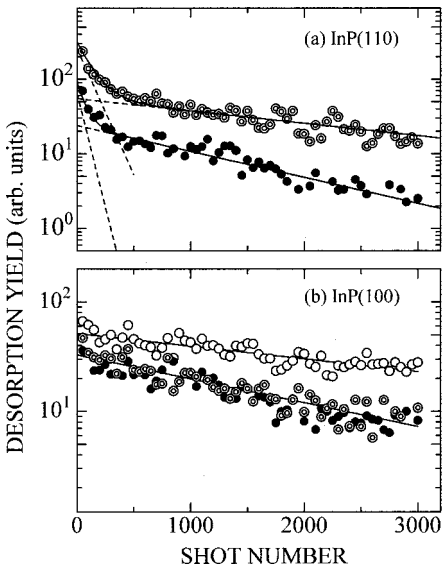

FIG. 4. Yields of desorption of (a) P_2 (◎) and In (●) from InP (110)-(1×1) and of (b) P (○), P_2 (◎), and In (●) from InP (100)-(4×2), induced by repeated irradiation of 460-nm laser pulses. The solid lines in (b) are the fit of the exponential decay to data. For P_2 and In from InP (110)-(1×1) in (a), two decay components (broken lines) are distinguishable, and the sum of the two components are shown by solid curves.

for each of the two surfaces. Figure 4 shows the results for InP(110) and InP(100); it is clear from the results that the yields of all species decrease with increasing n. In the case of InP(100), the decrease of each product can be fitted by a single straight line in the semilogarithmic plot; the yield Y_n by the nth pulse of irradiation decreases exponentially as a function of n, namely, $\ln(Y_n)=\ln(Y_1)-\alpha(n-1)$. The constant α which is referred to as the reduction constant, characterizes reduction of the desorption yield under a repeated irradiation. On the other hand, in the case of InP(110), the decrease in the yields of both P_2 and In can be fitted to the sum of two decreasing components with different α's which are shown by broken lines. We call hereafter the two the fast and slow components, respectively. For the InP(110) surface, similar measurements were made for different laser fluences for surface excitation. Although we could not determine the reduction constant for the fast component precisely, the constant α_s for the slow component was determined as a function of laser fluence Φ. The result shown in Fig. 5 indicates that α_s is proportional to Φ with different proportionality constants for P_2 and In. Quantitative analysis of this result of α's are given later in Sec. IV B.

As seen in Fig. 4, the fast decay of the yields of neutral desorbed species for InP(110) is completed within $n=500$. The reduction of the slow component of P_2 was at most 10% for another 1000 shots after irradiating the virgin spot of the surface with the first 500 shots, even for the highest fluence of 63 mJ/cm^2. This slow reduction of yields in this range ($n>500$) provides us a better chance for studying several important properties of desorption, since there is the condition of a quasiconstant rate of desorption with respect to the shot number. Based on this result, we first excited the fresh

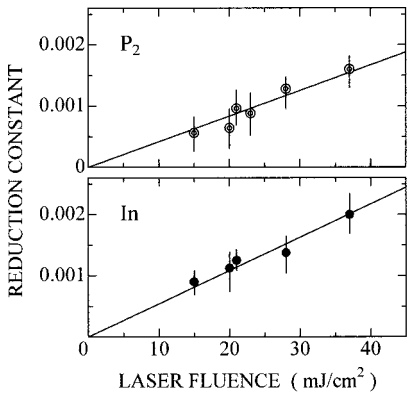

FIG. 5. Reduction constants for P_2 (◎) and In (●) from InP (110)-(1×1) as a function of fluence of 460-nm laser pulses for surface excitation.

spots of the surface with 500 laser shots of the same fluence to establish a similar surface condition for desorption. Changing the spots of the surfaces caused little effect on the desorption level after 500 shots. A similar surface treatment of preirradiation was applied also for the InP(100) surface. Then three different types of measurements were carried out for the surfaces treated by the preirradiation of 500 shots.

After the surface treatment with preirradiation, yields of desorption were measured as a function of fluence; the yields were determined as an average of 100 laser pulses with a given fluence. The results for InP(110) and InP(100) are shown in Figs. 6(a) and 6(b), respectively. It is evident in the figure that the yields of the three products show a superlinear dependence on the fluence, as has been reported for other semiconductor surfaces in previous studies. The solid curves in the figures are the calculated results of the model, which will be discussed below.

By applying the same surface treatment, we measured TOF spectra for P, P_2, and In desorbed from InP surfaces. In

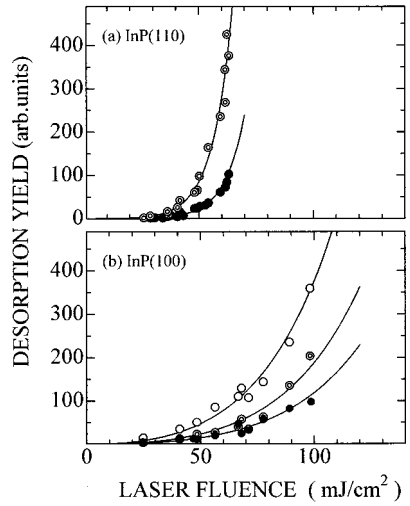

FIG. 6. Desorption yields of (a) P_2 (◎) and In (●) from InP (110)-(1×1) and those of (b) P (○), P_2 (◎), and In (●) from InP (100)-(4×2) as a function of fluence of 460-nm laser pulses. The solid curves are the best fit of the theoretical model of the two-hole localization (see text).

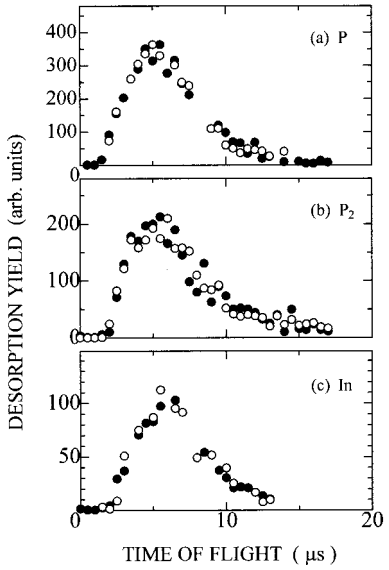

FIG. 7. Time-of-flight spectra of (a) P, (b) P_2, and (c) In, fron InP (100)-(4×2) desorbed by exciting the surface by 460-nm laser pulses. Open circles are the data for fluence of 40 mJ/cm^2, while solid circles are those for fluence of 98 mJ/cm^2. The data for fluence of 40 mJ/cm^2 were multiplied by appropriate factors to have similar peak heights to those of 98 mJ/cm^2.

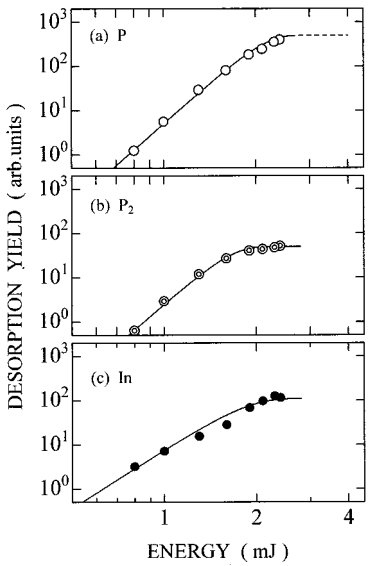

FIG. 8. Intensities of ion signals of (a) P, (b) P_2, and (c) In desorbed from InP (100)-(4×2) measured as a function of ionization-laser intensity scaled in terms of pulse energy. Signals of P_2 and In are almost saturated at energy of 2 mJ, while that of P still continues to grow at energy of 2 mJ.

this measurement, desorption yields were measured for a given fluence as a function of the time delay between the laser pulses for surface excitation and femtosecond laser pulses for ionization. The TOF spectra thus measured for InP(100) are shown in Fig. 7; two different symbols in the figure correspond to the results for two different fluences of excitation laser pulses. The spectrum for P is characterized by the peak flight time of 5 μs, that for P_2 by the time of 5.5 μs, and that for In by the time of about 6 μs. It is evident that not only the peak flight time but also the distribution is not dependent on the fluence of excitation laser pulses within the present experimental accuracy. Measurements of TOF spectra for P_2 and In from InP(110) have given similar features as those shown in Fig. 7; the peak flight times are essentially the same as those from InP(100), and no fluence-dependent peak flight times are detected.

In the present detection of neutral species by means of FNRIS, the technique measures the densities of desorbed species, not the flux as in the case of QMS measurements. Therefore, two factors should be taken into account for evaluating the desorption yield; one is the time of flight of each species with different masses from the surface to the ionization region, and the other is the ionization probabilities of species that have different ionization potentials. As seen in Fig. 7, all TOF spectra of P, P_2, and In have maxima around 5.5 μs after surface excitation, and the widths of TOF spectra are similar. Therefore, the mass spectra measured at time delay of 5.5 μs are representative of relative yields of the three species, except for the difference in ionization probabilities. In order to examine the difference in ionization probabilities of P, P_2, and In, we measured the ion signals of desorbed species as a function of intensity I_f of femtosecond laser pulses. The results are shown in Fig. 8 for P, P_2, and In from InP(100)-(4×2). Reflecting the difference in ionization potentials of the three species, the results shown in Fig. 8 show characteristic changes. For In, which has the smallest ionization potential of 5.78 eV, the signal increases proportionally to the fourth power of I_f in the weak power region, while it is saturated above I_f of 2 mJ. On the other hand, P and P_2 signals show a stronger dependence upon I_f (roughly proportional to sixth or seventh power of I_f) for the weak power region. The P_2 signal is almost saturated above 2 mJ of I_f, while the P signal continues to grow above I_f of 2 mJ. Therefore, we are detecting P_2 and In with an ionization probability of almost unity, but the yield of P atoms is underestimated (roughly 60%) at the present power level of the femtosecond laser pulses.

IV. DISCUSSION

A. Qualitative features of the desorption studied with a highly sensitive detection method

1. Electronic bond breaking as the origin of desorption

As described in Sec. III, we could detect neutral desorbed species simultaneously with sensitivity that is much higher than that in previous studies of LSD on compound semiconductor surfaces. The species detected are P_2 and In for InP(110) and P, P_2, and In for InP(100). Although these species have been detected previously, the most significant feature revealed in this study is the fact that the yields of these species depend strongly on surfaces properties. As described in Sec. III, the present method of detecting neutral species is essentially a density detection. However, consideration of TOF spectra of P, P_2, and In shown in Fig. 7 and of specimen-dependent ionization probabilities shown in Fig. 8 allows us to conclude that P_2 and In are the main products

of desorption for InP(110), while P, P_2, and In are desorbed from the InP(100) surface. Namiki, Cho, and Ichige[5] found that the fluence dependence of the yield of P_2 was identical for the two different surfaces of (110) and (100) of GaP. However, as demonstrated here, P_2 is the major product for InP(110), while monatomic P is that for InP(100). Also, the fluence dependence of the yields of neutral species shows clear differences for the two surfaces as seen in Fig. 6. Therefore, the present results, showing a strong contrast to the results of previous studies, indicate clearly that the desorption process at InP surfaces is strongly sensitive to surface structure when fluences are well below melt and ablation thresholds and the sensitivity of detection of neutral species is sufficiently high.

The TOF spectrum measured for P for InP(100)-(4×2) shows a peak flight time of 5.0 μs, which corresponds to the translational energy of 0.026 eV. The corresponding energies of 0.052 and 0.078 eV are evaluated from the TOF spectra for P_2 and In. An important feature seen in TOF spectra is that neither the peak-flight time nor the velocity distribution are dependent on the fluence of the excitation-laser pulse, although the yields change by a factor of 10 for the two fluences at which TOF spectra are measured. The amount desorbed per a single laser shot can be estimated to be at most 10^{-4} ML in the present study, since the maximum of the ion signals is at most 10^3 times larger than the detection limit that corresponds to 10^{-7} ML. For such number densities of desorbed neutral species, any effects of gas-phase collision may be neglected.[12] Therefore, we conclude that the velocity distributions shown in Fig. 7 are characteristic of the desorption processes of each respective species.

This fluence-independent velocity distribution shows a strong contrast to those obtained in the previous studies of LSD from *MX* compound semiconductors, in which fluence-dependent translational energies were often observed. In the case of sublimation from the molten layers on the surfaces, the translational energy increases with increasing fluence, as evidenced by the studies of laser annealing of semiconductor surfaces.[3] Therefore, we conclude that the LSD from InP surfaces in the present study is not due to laser-induced melting. Brewer, Zinck, and Olson[6] have studied the laser-induced desorption from CdTe with fluences below the melt threshold. They have shown that the velocity distribution is well described by a single Maxwellian component, with translational energy essentially identical to the surface temperatures calculated using one-dimensional heat-flow model, and that both Cd and Te_2 have the same translational energy. Based on these results, they concluded that a thermal mechanism was responsible for desorption of Cd and Te_2 under laser irradiation. However, in the present case, the velocity distribution and most probable translational energy are not dependent on fluence, and P, P_2, and In have different translational energies. Therefore, we conclude that the desorption process is not due to a thermal mechanism but is electronic in nature. Possible mechanisms of this electronic desorption will be discussed later in Sec. IV B.

2. Reactive sites and optical transition

The superlinear dependence of desorption yields shown in Fig. 6 and the decreasing yields with increasing shot number, or dose, shown in Fig. 4 are two additional phenomena that are characteristic of electronic desorption from InP surfaces. The latter observation of decreasing yield with increasing dose has been observed in previous studies by means of highly sensitive detection of neutral species.[7,8,13] This behavior of decreasing yields with increasing dose has been regarded as a piece of evidence that the reactive site of desorption is an atomic-scale defect on the surface. Although defect sites have not been identified in many cases, Yu and Tanimura have demonstrated that the Si ad-dimers on Si(100)-(2×1) with a surface concentration less than 0.1 ML provides the reactive site for desorption, and that the yield of Si-atom desorption decreases with increasing the number of laser shots at the same spot of the surface.[19] On the other hand, in the case where the intrinsic atomic site of the surface reconstructed structure acts as the reactive site for desorption, the yield is constant at least for the number of laser shots of 10^4, as shown by Ishikawa *et al.* for Si(111)-(7×7).[20] Based on these previous results, we conclude that the reactive sites of desorption on InP surfaces are atomic-scale defects on the surfaces.

For electronic bond breaking at a defect site, two modes of optical transition can be responsible; one is the direct optical excitation of a defect-associated localized electronic state, and the other is bulk and/or surface electronic transitions resulting in the formation of delocalized excited states followed by their localization onto the defect site. The superlinear dependent yield on excitation intensity is an essential feature in either case. The former direct defect excitation has been assumed in a literature, and the superlinearly dependent yield as a function of the excitation intensity has been ascribed to the multistep photoabsorption of defects, starting from the ground electronic state to the final''antibonding state'' via several intermediate excited-state configurations.[7] However, we conclude here that this is not the case in the electronic desorption from InP surfaces based on the results shown in Figs. 4 and 6. In these figures, we clearly see that all neutral species P_2 and In for InP(110) and P, P_2, and In for InP(100) show decreasing yields with different reduction constants and that the desorption yields of all species depend superlinearly on the fluence of excitation laser light. If the multistep photoabsorption of defects is responsible for the desorption, then we have to assume that all surface defects acting as reactive sites for different desorbed species have optical absorption bands at exactly the same wavelength of 460 nm for their ground and all intermediate states before reaching the final antibonding states. Furthermore, we have to assume that the width of such optical absorption bands are extremely wide, more than 1 eV, since similar decreasing yields have been observed for InP(100) surfaces excited with 337-nm photons.[13] Such a situation is very improbable, even unreasonable. On the other hand, as discussed in the next paragraph, an alternative model of nonlinear localization of surface excited species at the respective reactive sites describes reasonably and satisfactorily all of the important features of the electronic desorption from InP surfaces revealed in this study.

B. Model of electronic desorption on semiconductor surfaces; nonlinear localization of surface-excited species

1. Analysis of decreasing yields of desorption

The yield of electronic desorption of a particular species is proportional to the number density N of the reactive site from which atoms are removed and to the rate g of electronic bond breaking that takes place at certain excited states at the site. For a given g, we can define the reduction factor $\eta_n(g)$ for N upon the nth irradiation as

$$N_n = \eta_n(g) N_{n-1}, \tag{1}$$

where N_n is the number density of the site after the nth irradiation of laser pulses. Then the yield Y_n of desorption induced by the nth irradiation can be written as

$$Y_n = A N_{n-1} = A \prod_{i=1}^{n-1} \eta_i(g) N_0, \tag{2}$$

where A is a constant that correlates the desorption yield with the number density of the reactive site on the surface. When η_n is not dependent on n, Y_n is simply given by $Y_n = A N_0 \{\eta(g)\}^{n-1}$, leading to the linear relation between $\ln(Y_n)$ and $n-1$. When we define $\alpha = -\ln \eta$, then this linear relation is in fact observed in Fig. 5, although we need to introduce two sets of parameters that represent the fast and slow components for InP(110).

For obtaining deeper insight into the reduction factor, we follow the rate-equation model developed in Ref. 17. In this model, the rate of exciting reactive sites is treated in a phenomenological way in terms of the effective excitation cross section σ^*, and the desorption is assumed to be induced at an excited state of the reactive site with a probability that is superlinear with respect to the laser flux. The rate equations for the ground N_g and the excited N^* states of the reactive site are given by

$$\frac{dN^*}{dt} = \sigma^* \phi N_g - K_0 N^* - g(\phi) N^*, \tag{3}$$

$$\frac{dN_g}{dt} = -\sigma^* \phi N_g + K_1 N^*. \tag{4}$$

In these equations, ϕ is the flux of the excitation-laser pulse, K_0 the sum of all possible channels of the first-order decays at the excited state, including the deexcitation with the rate K_1 into the original ground state, and $g(\phi)$ is a function that characterizes the superlinear dependence on ϕ for desorption. The yield of the desorption, which has been measured as a time-integrated quantity over the temporal width t_0 of the excitation-laser pulse, is given by

$$Y = \int_0^{t_0} g(\phi) N^* dt. \tag{5}$$

For simplicity, a rectangular shape of the excitation-laser pulse is assumed, with a constant flux ϕ and a width t_0, namely $\Phi = \phi t_0$. For a much shorter lifetime of N^* compared with the pulse width t_0 (long-pulse approximation), the above equations are easily solved to give

$$N_g(t) = N_g^0 \exp\left[-\sigma^* \phi \left(1 - \frac{K_1}{K_0 + g(\phi)} \right) t \right], \tag{6}$$

$$Y = \frac{g(\phi)}{K_0 - K_1 + g(\phi)} \{ N_g^0 - N_g(t_0) \}. \tag{7}$$

In view of the results of this rate-equation model, number density of the reactive site at the end of a pulse is given by $N_g(t_0)$. Therefore, the reduction factor is given by $\eta = \exp(-\sigma^* \phi t_0 \{1 - K_1/[K_0 + g(\phi)]\})$. As shown in Fig. 5, a linear relation holds between $-\ln \eta$ and Φ $(= \phi t_0)$ for desorption of both P_2 and In. Then, $K_0 \gg g(\phi)$ or $K_1, K_0 \ll g(\phi)$ must hold, together with σ^*, which is not dependent on ϕ. However, if the latter is the case, then we have, from Eq. (8), $Y_n \approx (1-\eta) N_{n-1}$, which does not show any superlinear dependence on the fluence. It follows that $K_0 \gg g(\phi)$; the first-order decay channels dominate over the desorption in the deexcitation process of the excited state of the reactive site. This is an important consequence deduced from the analysis in terms of the phenomenological rate-equation model.

2. Possible mechanism of superlinear dependence of the desorption yield

In view of the model of localization of excited states at the reactive site, the above-mentioned effective excitation cross section and the rate of desorption are formulated as follows. Let N_e be the concentration of surface excited species (electrons, holes, or excitons) generated by laser excitation. The rate equation for N_e is given by

$$\frac{dN_e}{dt} = \sigma \phi N_0 - \frac{1}{\tau} N_e - f(N_e), \tag{8}$$

where σ is the absorption cross section of photons of laser light, N_0 the density of state of the ground electronic state, τ the lifetime of the excited species, and $f(N_e)$ is a function that characterizes possible nonlinear decay channel of the excited species. When we assume that the monomolecular decay channel dominates over the nonlinear decay of the excited state,[21] then N_e is given by $N_e = \sigma \phi \tau N_0$ in the long-pulse approximation. The lifetime τ of the excited states is determined by all possible deexcitation channels, and it can be written generally as $1/\tau = 1/\tau_0 + \Gamma$, where Γ is the rate of trapping the excited state by surface defects, and $1/\tau_0$ is the total rate of deexcitation other than the trapping. The rate Γ can be written generally as

$$\Gamma = \gamma N_e N_g = (\sigma \tau \gamma N_0) \phi N_g, \tag{9}$$

where γ is a bimolecular reaction constant in the trapping process. Then the effective excitation cross section in Eq. (1) corresponds to $\sigma \tau \gamma N_0 (= \sigma^*)$ in this model.

The superlinear dependence of Y on Φ shown in Fig. 6 indicates that multiple photogenerated excited species are involved in the localization process. Among several excited species, the important role of surface holes has been empha-

sized. Sumi studied theoretically the two-hole localization as a possible mechanism of electronic desorption of constituents of semiconductor surfaces and formulated the rate J of the two-hole localization onto a particular lattice site.[22] His result of J for the successive capture of the second hole onto the first-hole localized site can be approximated well by $J = j_c\{\exp(n_h)-1\}^2 N_g$, where j_c is a constant, that depends on several properties of the reactive site. The quantity n_h is the concentration of photogenerated surface holes normalized to the effective number Z of free-hole states in the surface valence band at a given temperature. For the weak-excitation regime, J shows quadratic dependence on n_h, while it increases exponentially for the intense-excitation region.

In this two-hole localization scheme, the excited species described by Eq. (8) are the surface holes, and the excited state of the reactive site of Eqs. (3) and (4) is the first-hole localized state. The rate of two-hole localization formulated by Sumi corresponds exactly to the term $g(\phi)N^*$ in Eq. (3). Since the quantity n_h is given by

$$n_h = \sigma\Phi(\tau/t_0)N_0/Z, \tag{10}$$

in the long-pulse approximation, it is proportional to the excitation intensity characterized by Φ. Therefore, J is expressed as $J = J_0\{\exp(B\Phi)-1\}^2$, where J_0 is a constant. The experimental results of Y were compared with this equation with J_0 and B being fitting parameters. The solid curves in Fig. 6 are the best fit of this equation to experimental results; it is evident that it describes almost perfectly the results for a whole range of the excitation intensities for all desorbed species from two different surfaces. By considering possible differences in the magnitudes of j_c and N_g for respective reactive sites, the best-fit values of the J_0's are different for different species. However, the same value of B has been used for different desorbed species from the same surface, which is a requirement of the two-hole localization model.

It is now established that the surface relaxation on the InP(110) surface involves charge transfer from In-atom dangling bonds to P-atom dangling bonds, leading to the formation of quasi-one-dimensional rows of P atoms on the topmost layer.[23] The laser wavelength of 460 nm used in this study falls in resonance with the lowest surface transition band, which is characteristic of the relaxed (110) surface. Therefore, surface-excited species are generated in InP (110)-(1×1), together with bulk-excited states. Although the surface electronic structures of InP(100)-(4×2) have not yet been clarified, the surface transition energy may not be the same as those of InP(110)-(1×1) because of the more complicated reconstruction. As seen in Fig. 6, the desorption from InP(110) is more efficient than that from InP(100). This may be related to the difference in efficiencies of forming surface excited states that, in many cases, are effective in electronic bond breaking of covalent semiconductor surfaces.[8,9]

C. Reactive sites on InP(110)-(1×1) and InP(001)-(4×2)

As discussed above, all of the important features of electronic desorption from InP surfaces have been described satisfactorily by the model of two-hole localization of surface holes at surface defects. Although LEED measurements confirmed the well-ordered (1×1) and (4×2) periodic structures of the surfaces used in this study, atomic-scale defects of several forms may exist on the surfaces. Here we briefly discuss the surface defects as the possible reactive sites on the InP surfaces. First, we make a rough estimate of the amount of defects involved in the desorption process studied here. Based on the detection sensitivity mentioned in Sec. III and the highest signal detected by FNRIS, we estimate the total amount of P_2 molecules, which is the main product of the desorption from InP(110)-(1×1), to be about 1×10^{-4} ML. As discussed in Sec. IV B, the rate of monomolecular processes at the defect excited states is much higher than the rate of desorption. When we assume the rate $K_0 - K_1$ responsible for the monomolecular decay is higher by a factor of 100 than the rate of desorption, then the initial concentration of the reactive sites is estimated to be 0.01 ML. This amount of defects on the reconstructed surface may be well expected.

One possible source of defects may come from the process of preparing the surfaces; InP surfaces in the present study were prepared by several cycles of cleaning processes of Al^+ sputtering and thermal annealing. For (110) surfaces of III-V semiconductors, it has been shown that dimer configurations of nonmetallic atoms are often induced when the surface is heated to a certain temperature below melting.[24] Therefore, it is presumed that such P_2-type defects are frozen on the present (110) surface. On the other hand, InP (100)-(4×2) has been shown to be In-rich.[25,26] Therefore, the formation of dimer P atoms may be suppressed, compared to the stoichiometric (110) surface, and monatomic P-type defects could be formed. Significant differences of the yields of desorbed species for the two surfaces may be caused by the difference in stoichiometry of the two surfaces. The other possible source of generating defects on the surfaces may be the electronic process induced by LEED and AES measurements for characterizing our surfaces. Recently, scanning tunneling microscopy (STM) has been used to study structural changes on semiconductor surfaces induced by electron and laser irradiation. For GaAs surfaces, which were prepared by cleaving under ultrahigh vacuum condition, it has been shown that electrons of the sort used in AES and LEED cause surface point defects.[10] Electronic processes may be expected on our InP surfaces to generate surface defects similar to the reactive sites for desorption.

It has also been shown that laser-light irradiation of GaAs(110)-(1×1) surfaces with defects modifies strongly their morphologies.[10,27] Since InP(110)-(1×1) has features similar to those of GaAs(110)-(1×1), excitation-induced defect processes on InP(110)-(1×1) may well be presumed. These excitation-induced defect reactions on surfaces may be related strongly to the desorption of neutral species of P, P_2, and In. In the study of laser-induced desorption of Si atoms from Si(111)-(7×7), it has been shown that electronic bond breaking of adatoms leads directly to the formation of adatom vacancies and to Si-atom desorption at an electronically ground state.[9] STM observation of irradiated surfaces has revealed that adatom vacancies thus created are mostly in the form of the monovacancy, and that no Si-atom aggregates

are formed on the surface for the defect level below 10%.[9] Therefore, laser irradiation does not induce any complicated photon-assisted reactions of surface defects that are generated by laser-induced electronic processes on Si (111) -(7×7). However, the atomic processes on compound semiconductor surfaces under laser irradiation may be more complicated; laser irradiation induces changes in defect morphologies on one side and causes desorption of neutral atoms on the other side.

As discussed in Sec. IV B, the dominant channel of monomolecular decay of defect excited states is involved in the electronic desorption. It is this monomolecular process that governs the decrease in the number density of reactive sites. We speculate that the monomolecular decay of the defect excited states corresponds to the changes in defect morphologies (via photoactivated defect reactions on the surface) into some forms which no longer be active for the desorption. Such defect reactions may be sensitive to the initial conditions of the surface in terms of the stoichiometry, the morphologies of existing defects, and their number densities. Therefore, the direct correlation may not be possible at this moment between the reactive sites of desorption on InP surfaces used in this study and previously obtained knowledge of surface defects in atomic levels on similar surfaces that are prepared by different methods to have very low defect concentrations.

It is evident that definite identification of reactive sites of laser-induced electronic desorption can be possible only by combining atomic-scale knowledge of surface structures under laser irradiation with results of highly sensitive detection of desorbed species. In the previous studies of LSD by means of QMS, such a microscopic knowledge of surface defects of atomic levels cannot be the subject of discussion, since desorption always occurs at highly damaged layers. Our method of FNRIS, which makes it possible to detect desorbed neutral species simultaneously with a high sensitivity of the 10^{-7} ML, has opened a new stage in the research of LSD to understand the processes from a microscopic viewpoint of the atomic level. Such a comprehensive study by combining STM observation of irradiated surfaces with highly sensitive simultaneous detection of desorbed species by FNRIS is now underway.

V. SUMMARY

In this paper, we have studied laser-induced electronic desorption from surfaces of InP(110)-(1×1) and InP (100)-(4×2) for laser fluences well below the melt and ablation thresholds. We have demonstrated that the method of FNRIS is useful for detecting desorbed neutral species simultaneously with a high sensitivity of 10^{-7} ML per pulse. For InP(110)-(1×1) and InP(100)-(4×2), species desorbed are P, P_2, and In, the relative yields of which are strongly dependent on the surface structures. The P_2 molecules are desorbed predominantly from InP(110)-(1×1), while monatomic P is the main product of desorption from InP(100)-(4×2). As the characteristics of the electronic desorption, it has been shown that the efficiencies of desorption for the three species depend superlinearly on the excitation intensity, and that the yields of desorption of all species decrease with increasing number of laser shots on the same spot. We have concluded that the desorption takes place at the reactive sites of preexisting surface defects. As the mechanism of the laser-induced desorption on InP surfaces, we have proposed the mechanism of two-hole localization at defect sites, which can explain most of the features of the desorption processes revealed in this study. The atomistic identification of the reactive sites on the surfaces has been left as an important future problem.

ACKNOWLEDGMENT

Support of this research by Grant-in-Aid for Scientific Research by the Ministry of Education, Science, Sports and Culture of Japan is gratefully acknowledged.

*Present address: Department of Intelligent Materials Engineering, Osaka City University, 3-3-138 Sugimoto, Sumiyoshi, Osaka 558-8585, Japan.

†Present address: The Institute of Scientific and Industrial Research, Osaka University, 8-1 Mihogaoka, Ibaraki, 567-0047, Japan.

[1] M. Von Allmen, *Laser-Beam Interaction with Materials; Principles and Applications* (Springer, Berlin, 1995).

[2] D. von der Linde, in *Ultrashort Laser Pulses*, edited by W. Kaiser (Springer, Berlin, 1988).

[3] B. Stritzker, A. Pospieszczyk, and J. A. Tagle, Phys. Rev. Lett. **47**, 356 (1981).

[4] N. Itoh and T. Nakayama, Phys. Lett. A **92A**, 471 (1982); T. Nakayama, Surf. Sci. **133**, 101 (1983).

[5] A. Namiki, S. Cho, and K. Ichige, Jpn. J. Appl. Phys., Part 1 **26**, 39 (1987).

[6] P. D. Brewer, J. J. Zinck, and G. L. Olson, Appl. Phys. Lett. **57**, 2526 (1990).

[7] K. Hattori, A. Okano, Y. Nakai, and N. Itoh, Phys. Rev. B **45**, 8424 (1992).

[8] J. Kanasaki, A. Okano, K. Ishikawa, Y. Nakai, and N. Itoh, Phys. Rev. Lett. **70**, 2495 (1993).

[9] J. Kanasaki, T. Ishida, K. Ishikawa, and K. Tanimura, Phys. Rev. Lett. **80**, 4080 (1998); J. Kanasaki, K. Iwata, and K. Tanimura, *ibid.* **82**, 644 (1999).

[10] K. Nakayama and J. H. Weaver, Phys. Rev. Lett. **82**, 980 (1999); B. Y. Han, K. Nakayama, and J. H. Weaver, Phys. Rev. B **60**, 13 846 (1999).

[11] *Desorption Induced by Electronic Transitions I*, edited by N. H. Tolk, M. M. Traum, J. C. Tully, and T. E. Madey (Springer, Berlin, 1983).

[12] R. Kelly and R. W. Dreyfus, Nucl. Instrum. Methods Phys. Res. B **32**, 341 (1988).

[13] B. Dubreuil and T. Gilbert, J. Appl. Phys. **76**, 7545 (1994).

[14] M. L. Wise, A. Bruce Emerson, and S. W. Downey, Anal. Chem. **67**, 4033 (1995).

[15] G. K. Nicolussi, M. J. Pellin, K. R. Lykke, J. L. Trevor, D. E. Mencer, and A. M. Davis, Surf. Interface Anal. **24**, 363 (1996).

[16] V. L. Berkovits, L. F. Ivantsov, I. V. Makarenko, T. A. Minashvili, and V. I. Safariv, Solid State Commun. **64**, 767 (1987).

[17] S. Selci, A. Cricenti, A. C. Felici, C. Goletti, and G. Chiarotti, Phys. Rev. B **44**, 8327 (1991).

[18] For evaluating ρ, we introduce a mean velocity v_0 and a width W ($v_0 \approx W/2$) for a rectangular form of velocity distribution of desorbed neutrals. At a time delay t, neutral species with a velocity v arrive at the center of the ionization volume which is separated from the surface by the distance L: $v = L/t$. Because of the finite size of the ionization volume, which is characterized by the diameter d of the volume, neutral species with velocities $v + \delta v$ are present in the ionization volume at the delay time. For the time delay t_0, when the central part of the velocity distribution arrives at the center of the volume, δv is given by $\delta v = \delta L/t_0$, where $t_0 = L/v_0$. Since $\delta L = d$, the fraction can be evaluated as $\rho = \delta v/W = (v_0/W)(d/L)$. Under the present experimental condition that $d = 0.2$ mm and $L = 2$ mm, we can estimate that $\rho \approx 0.05$.

[19] I.-K. Yu and K. Tanimura, Solid State Commun. **101**, 429 (1997).

[20] K. Ishikawa, J. Kanasaki, Y. Nakai, and N. Itoh, Surf. Sci. Lett. **349**, L153 (1996).

[21] As shown by the analysis of the results in Fig. 5, the effective excitation cross section σ^* is not dependent on the excitation laser intensity ϕ. If the nonlinear decay process of the excited state is significant, then we have solutions of N_e, which is nonlinearly dependent on ϕ. In such a case, we have fluence-dependent σ^*, which is not consistent with the results. Therefore, the first-order decay should be assumed to be much larger than the nonlinear decay of the excited species. This is not at all contradictory to the idea of two-hole localization, since two-hole localization is assumed to take place successively, not simultaneously. The successive capture of the second hole by the first-hole localized site can be treated in the frame of monomolecular decay of the excited species (Ref. 22).

[22] H. Sumi, Surf. Sci. **248**, 382 (1991).

[23] W. Monch, *Semiconductor Surfaces and Interfaces* (Springer, Berlin, 1995).

[24] F. Proix, A. Akremi, and Z. T. Zong, J. Phys. C **16**, 5449 (1983).

[25] M. D. Pashley, K. W. Haberem, W. Friday, J. M. Woodall, and P. D. Kirchner, Phys. Rev. Lett. **60**, 2176 (1988).

[26] M. M. Sung, C. Kim, H. Bu, D. S. Karpuzov, and J. W. Rabalais, Surf. Sci. **322**, 116 (1995).

[27] J. P. Long, S. S. Goldenberg, and M. N. Kabler, Phys. Rev. Lett. **68**, 1014 (1992).